Visualizing Non-Equilibrium Flow Simulations using 3-D Velocity Distribution Functions

A. Venkattraman and A.A. Alexeenko

School of Aeronautics & Astronautics, Purdue University, West Lafayette IN 47907

Abstract. Scientific visualization techniques have been used to probe and understand better the physics of non-equilibrium flows. A visualization methodology for non-equilibrium flow simulations using 3-D velocity distribution functions(VDFs) is illustrated in application to various non-equilibrium flow problems. A one-dimensional normal shock wave problem is considered for two different upstream Mach numbers corresponding to weak and strong non-equilibrium flow conditions. The iso-surfaces of 3-D VDFs inside the shock wave obtained using various solution techniques including the ES-BGK method, DSMC technique, Mott-Smith solution, and the Navier-Stokes(NS) distribution functions using Chapman-Enskog theory are compared and contrasted. The visualization technique is extended to two-dimensional hypersonic flow at $M = 10$ past a flat plate with sharp leading edge by comparing the isosurfaces of 3-D NS VDFs obtained at three different locations in the flowfield. The visualization of 3-D VDFs is shown to provide valuable information about the degree and direction of non-equilibrium for both 1-D and 2-D flows.

Keywords: direct simulation Monte Carlo; velocity distribution functions; rarefied flows; non-equilibrium flows; visualization

1. INTRODUCTION

Visualization plays a very important role in the analysis and interpretation of numerical solutions. The development of flow visualization techniques and tools for rendering scalar, vector and tensor fields obtained by Computational Fluid Dynamics (CFD) techniques has significantly accelerated the adaptation of CFD in many areas of science and engineering[1]. Visualizing higher-dimensional (> 3D) data has been an active research area[2, 3] in order to design methods that overcome the difficulties involved in representing such data on a two-dimensional computer screen. Higher-dimensional data occur in a wide range of applications including medical imaging, uncertainty visualization and fluid flows. Non-Equilibrium flows that are encountered in a number of flows including supersonic flight at high altitudes, flows expanding into vacuum and flows in microscale devices are governed by the Boltzmann equation[4]

$$\frac{\partial}{\partial t}(nf) + \mathbf{c} \cdot \frac{\partial}{\partial \mathbf{x}}(nf) = \int_{-\infty}^{\infty} \int_{0}^{4\pi} n^2 (f^* f_1^* - f f_1) c_r \sigma d\Omega d\mathbf{c_1} \tag{1}$$

where f is the velocity distribution function(VDF) that depends on 7 independent variables - time, 3 physical coordinates, and 3 velocity coordinates - and for a general three-dimensional flow problem. Unlike continuum equations, like the Navier-Stokes equations, which are in terms of macroscopic parameters including density, velocity, temperature and pressure, the Boltzmann equation is in terms of the velocity distribution function. In spite of the VDF being the fundamental quantity of interest, visualization techniques applied to non-equilibrium flow problems solved using the Boltzmann equation and its approximations have been restricted to macroscopic parameters mainly due to the high dimensional nature of the VDF. The macroscopic parameters, which are moments of the VDF, do not completely describe the features of non-equilibrium flows. The main goal of this paper is to study the distinguishing features of non-equilibrium flows by probing the VDF using visualization techniques for 3-D scalar fields. In particular, the structure of a normal shock wave is considered and VDFs inside normal shock waves obtained using various solution techniques are visualized. Later, the VDFs at various locations of two-dimensional hypersonic flow past a flat plate at $M = 10$ are presented. The remainder of the paper is organized as follows. Section 2 briefly provides the necessary theory & background including the numerical and visualization techniques used; Section 3 presents the results and discusses the same with Section 4 reserved for conclusions.

2. THEORY & BACKGROUND

The Boltzmann equation in its original form is often very difficult to solve due to its non-linear integro differential collision term. Non-equilibrium flows that are governed by the Boltzmann equation are typically solved using approximations to the original Boltzmann equation or by resorting to statistical techniques like the direct simulation Monte Carlo (DSMC) technique. Most of the approximate methods make an assumption for the form of the distribution function. Some of the popular forms for the non-equilibrium distribution function are briefly described below.

Equilibrium Maxwellian Distribution Function

The VDF in equilibrium flow conditions is the Maxwellian or isotropic Gaussian given by

$$f_M = \frac{\beta^3}{\pi^{3/2}} \exp[-\beta^2((c_x-u)^2+(c_y-v)^2+(c_z-w)^2)] \tag{2}$$

where u, v, and w are the mean velocities in the x, y, and z directions respectively. $\beta = (2RT)^{-1/2}$ with T being the local temperature and R the specific gas constant.

Relaxation to Anisotropic Gaussian Distribution : ES-BGK

A popular technique used to solve the Boltzmann equation is the use of model kinetic equations in which the complex collision term in the right hand side of the Boltzmann equation is replaced with a relaxation-type term and given by

$$\frac{\partial}{\partial t}(nf) + \mathbf{c}\cdot\frac{\partial}{\partial \mathbf{x}}(nf) = -\nu(f-f_0) \tag{3}$$

For the ellipsoidal statistical Bhatnagar-Gross-Krook (ES-BGK) equation[5], the VDF relaxes towards an anisotropic Gaussian[6] given by.

$$f_0 = \frac{\rho}{\sqrt{det(2\pi\mathbb{T})}} e^{\left[-\frac{1}{2}(\vec{c}-\vec{c}_0)^T\mathbb{T}^{-1}(\vec{c}-\vec{c}_0)\right]} \tag{4}$$

where,

$$\rho\mathbb{T} = \frac{1}{Pr}\rho RTI + \left(1-\frac{1}{Pr}\right)\rho\Theta; \rho\Theta = <(\vec{c}-\vec{c}_0)\otimes(\vec{c}-\vec{c}_0)f>$$

where ρ is the density, R is the specific gas constant, $\mathbf{c}_0$ is the mean velocity vector.

Navier-Stokes Distribution Function : Chapman-Enskog Theory

An approximation to the Boltzmann equation for very small perturbations from equilibrium conditions was developed using a first order approximation to the VDF based on the Chapman-Enskog theory[7] and is given by

$$f_{CE} = f_M\left(1-\frac{4\kappa\beta^2}{5\rho R}(\beta^2 c'^2 - 5/2)\mathbf{c}'\cdot\frac{\partial(\ln T)}{\partial \mathbf{x}} - \frac{4\mu\beta^4}{\rho}\mathbf{c}'^0\mathbf{c}' : \frac{\partial \mathbf{c}_0}{\partial \mathbf{x}}\right) \tag{5}$$

where f_M is the equilibrium Maxwellian distribution function at the local flow conditions, ρ is the density, $\mathbf{c}_0$ is the mean velocity vector, κ is the thermal conductivity with $\mathbf{c}'$ being the thermal velocity vector.

Bi-Modal Distribution Function : Mott-Smith Theory

Mott-Smith solution[4, 8] for the structure of a normal shock wave expresses the VDF at any location within the shock wave as a bi-modal distribution given by

$$n(x)f_{MS} = \frac{n_1}{1+\exp\{\alpha(x/\lambda_1)\}}f_{M1} + \frac{n_2\exp\{\alpha(x/\lambda_1)\}}{1+\exp\{\alpha(x/\lambda_1)\}}f_{M2} \tag{6}$$

where f_{M1} and f_{M2} are Maxwellian distributions corresponding to the upstream and downstream conditions of the shock wave. The density profile is then given by,

$$\frac{\rho}{\rho_1} = \frac{1+\exp\{\alpha(x/\lambda_1)\}\rho_2/\rho_1}{1+\exp\{\alpha(x/\lambda_1)\}} \tag{7}$$

Numerical & Visualization Methods

A finite volume scheme with third order accurate WENO scheme for spatial fluxes[9] is used to solve the ES-BGK model kinetic equations. The DSMC solutions were obtained using Bird's fortran code *DSMC1S.f* that is specialized

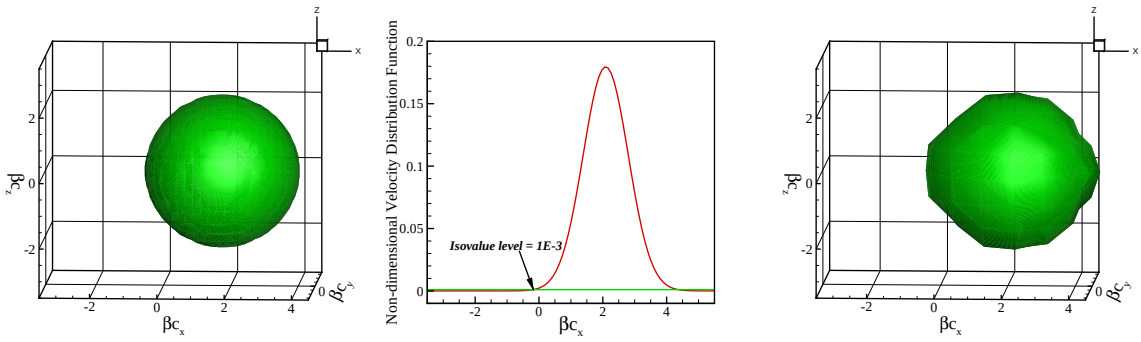

FIGURE 1. (Left) Isosurface of the maxwellian velocity distribution function corresponding to an isovalue of $\bar{f} = 1E-3$ using a $40 \times 26 \times 26$ velocity mesh, (middle) a 1-D maxwellian showing the isosurface level and (right) isosurface using a $10 \times 10 \times 10$ velocity mesh.

to solve the problem of a one-dimensional stationary shock wave. While the VDF is directly solved for in the ES-BGK method, the DSMC simulation requires the sampling of molecules to construct the 3-D VDF. The VDF obtained at a particular physical location is a 3-D scalar field that is a function of the velocity space coordinates. This 3-D scalar field is visualized using the classical technique of iso-surfacing. The shape of these iso-surfaces serves as an indicator of the degree and direction of non-equilibrium at that physical location.

3. RESULTS AND DISCUSSION

In this section, the classical non-equilibrium problem of the structure of stationary normal shock waves in Argon is considered for two upstream Mach numbers (M) corresponding to both weak (M=1.4) and strong non-equilibrium flow problems (M=2.5). Before proceeding further to probe the non-equilibrium flows, we present some iso-surfaces of the equilibrium Maxwellian distribution function that, in non-dimensional form, is given by

$$\bar{f}_M = \frac{1}{\pi^{3/2}} \exp[-\{(\bar{c}_x - \bar{u})^2 + (\bar{c}_y - \bar{v})^2 + (\bar{c}_z - \bar{w})^2\}] \tag{8}$$

All velocity components are non-dimensionalized by the local value of β and f is non-dimensionalized by β^3. The equation for the isosurfaces of the non-dimensional equilibrium Maxwellian distribution function $\bar{f}_M$ is given by

$$(\bar{c}_x - \bar{u})^2 + (\bar{c}_y - \bar{v})^2 + (\bar{c}_z - \bar{w})^2 = \text{constant} \tag{9}$$

with T being the local temperature. The maximum value of $\bar{f}_M$ occurs when $\bar{c}_x = u$, $\bar{c}_y = v$, and $\bar{c}_z = w$ and the maximum value is given by $\bar{f}_M = 1/\pi^{3/2}$. Figure 1 shows isosurfaces of the equilibrium Maxwellian distribution function corresponding to non-zero mean velocity in the x-direction for $\bar{f} = 1E-3$ and also the isovalue level on a 1-D maxwellian. Clearly, the iso-surfaces of $\bar{f}_M$ are spheres whose centre corresponds to the mean velocity of the flow at that physical location and whose radius depends on the iso-value chosen.

Weak Non-Equilibrium : M = 1.4

The weak non-equilibrium flow problem that has been considered is that of the structure of a normal shock wave in Argon at an upstream Mach number of 1.4. For both the ES-BGK method and the DSMC method, the number of cells in the physical space was fixed at 400. For the ES-BGK method, the number of grid points in the velocity space was $26 \times 16 \times 16$. Figure 2 shows the normalized density and temperature profiles obtained using the model kinetic equations, DSMC technique, and Mott-Smith theory. The macroscopic parameters obtained using the ES-BGK method agrees extremely well with that obtained using the DSMC technique while the Mott-Smith solution predicts a thicker shocker wave. The VDFs were constructed using various solutions including the direct simulation Monte Carlo (DSMC), model kinetic equations (ES-BGK), Navier-Stokes (NS) VDF from Chapman-Enskog theory, and the Mott-Smith theory. The NS distribution function was constructed using the shear stress and heat flux values obtained using the ES-BGK method. The number of molecules used to sample the 3-D distribution function from the DSMC simulation was about 65 million. Iso-surfaces of the non-dimensionalized velocity distribution function are visualized

in Figure 3 for $\bar{f} = 1E-3$ at the physical location corresponding to $x/\lambda = -2.0$. The distribution functions obtained using different methods look almost identical and deviate very little from the spherical isosurfaces of the equilibrium Maxwellian distribution.

Strong Non-Equilibrium : M = 2.5

In this section, we present results for a stronger shock wave in Argon with an upstream Mach number of $M = 2.5$. The number of cells in the physical space was fixed at 400 for both ES-BGK and DSMC methods. The number of grid points in the velocity space was fixed at $40 \times 26 \times 26$. Figure 4 shows the normalized density and temperature profiles obtained using the ES-BGK method, DSMC method and Mott-Smith theory. The macroscopic parameter profiles obtained using the ES-BGK and DSMC methods agree well except in a small region upstream of the shock wave in the normalized temperature profile. The Mott-Smith solution once again predicts a thicker shock wave. Figure 5 shows the iso-surfaces of non-dimensional VDF corresponding to an isovalue of $\bar{f} = 1E-3$ within the normal shock wave at the location $x/\lambda = -2.0$. The number of molecules used to sample the 3-D VDF from the DSMC simulation was about 70 million. Clearly, the VDFs deviate from the spherical Maxwellian distribution with an elongation along the x-direction indicating significant non-equilibrium along the x-direction. While the ES-BGK and Mott-Smith solutions predict strong and weak bimodal VDFs respectively, the DSMC method predicts a high eccentricity ellipsoidal isosurface for the VDF. The NS distribution function resembles the Mott-Smith distribution function but significantly underpredicts the fraction of molecules with a negative x-velocity. One of the reasons for the ES-BGK and DSMC methods predicting different VDFs upstream of the shock wave, in spite of excellent agreement in the macroscopic parameter profiles at $x/\lambda = -2.0$, is due to the fact that the ES-BGK method uses a collision frequency that is independent of the molecular velocities. Figure 6 compares the iso-surfaces for various values of the non-dimensional VDF obtained using the ES-BGK method. The presence of holes in the iso-surface at values of $\bar{f} <= 1E-6$ is related to the extent of the velocity domain used in the ES-BGK method. Decreasing the extent of the velocity domain would lead to the presence of holes for larger values of $\bar{f}$.

Two-Dimensional Hypersonic Flow

The visualization technique described above can be extended to two-dimensional flows with regions of non-equilibrium. We consider the two-dimensional hypersonic flow of cold nitrogen past a flat plate with a sharp leading edge at a freestream Mach number of $M = 10.0$. The freestream temperature is 47 K with the plate temperature fixed at 300 K. A Maxwell model was used for the gas-surface interaction with an energy accomodation coefficient of 0.75. The DSMC solver SMILE[10] is used to obtain the macroscopic parameters, the derivatives of which are used to construct NS VDFs using the Chapman-Enskog theory at three different locations in the flowfield. The density and temperature contours along with the three VDF locations in the flowfield are shown in Figure 7. Location 1 corresponds to a distance of $x/\lambda = 0.25$ from the sharp leading edge of the plate and is within the region of the flowfield where non-continuum effects are likely to play a significant role. Location 2 and 3 are further downstream at distances $x/\lambda = 17$ and $x/\lambda = 57$ respectively from the leading edge. Figure 8 compares isosurfaces of the NS VDFs corresponding to an isovalue of $\bar{f} = 1E-3$ for the three locations. Clearly, the maximum deviation from equilibrium is at location 1 where the VDFs show significant distortion in both x and y directions. The orientation of the isosurfaces along a direction that is neither along x-axis nor along y-axis clearly indicates the 2-D nature of non-equilibrium. The degree of non-equilibrium decreases as we move further downstream with the distortion of iso-surfaces decreasing as we move from location 1 to 3.

4. CONCLUSIONS

A visualization methodology has been proposed to visualize non-equilibrium flow simulations using 3-D VDFs. Results were presented for both 1-D and 2-D flow problems. A 1-D normal shock wave problem was considered for two different upstream Mach numbers $M = 1.4$ and $M = 2.5$. The iso-surfaces of the VDF at $x/\lambda = -2.0$ inside the shock wave obtained using various solution methods including the ES-BGK method, DSMC technique, Mott-Smith solution, and the Chapman-Enskog theory were presented. The isosurfaces of the distribution function obtained using various methods for the weak non-equilibrium case were almost identical whereas different methods gave significantly different isosurfaces for the strong non-equilibrium case. The differences can be attributed to fundamental assumptions associated with each of the methods including the form of the collision frequency. The technique was also used to visualize the Navier-Stokes velocity distibution functions at different locations in a 2-D hypersonic flow past a flat plate. The isosurfaces clearly indicate the 2-D nature of the non-equilibrium with distortions in both x and y directions with the distortion being maximum closest to the leading edge where the rarefaction effects are most significant. Hence, the visualization of VDF can provide valuable information about the degree and direction of non-equilibrium.

It can also be used to assess accuracy of the numerical solution with respect to grid resolution in the velocity space for deterministic solution techniques.

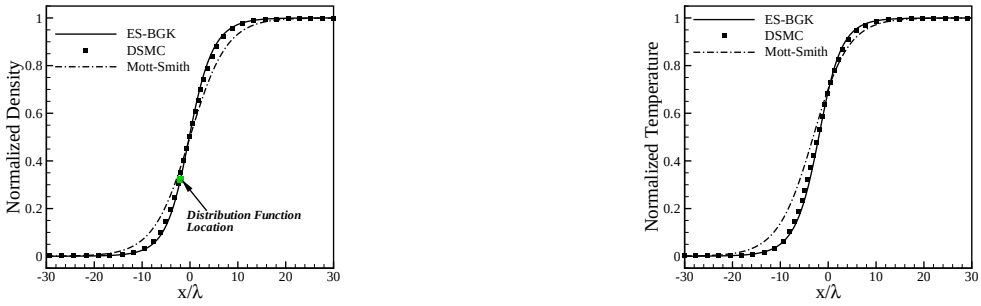

FIGURE 2. Comparison of normalized density and temperature profiles obtained using various methods for M = 1.4

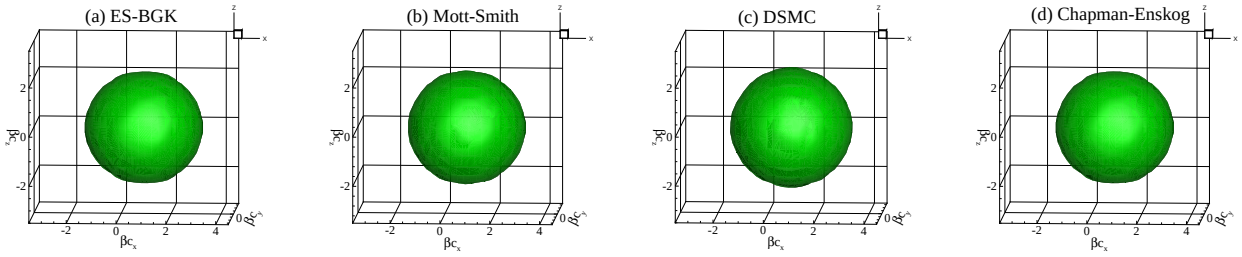

FIGURE 3. Iso-surfaces of the non-dimensional velocity distribution function within a normal shock wave with upstream Mach number $M = 1.4$ corresponding to an iso-value of $f = 1E-3$ obtained using various methods.

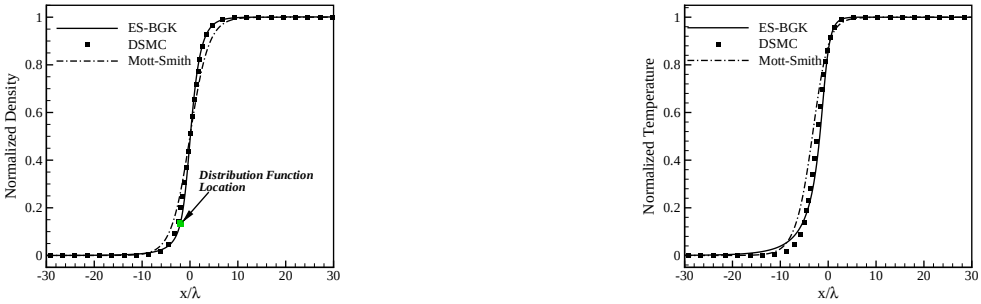

FIGURE 4. Comparison of normalized density and temperature profiles obtained using various methods for M = 2.5

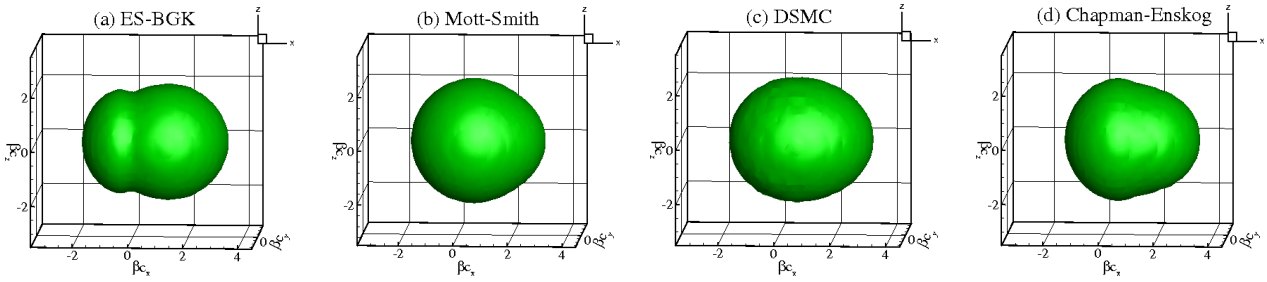

FIGURE 5. Iso-surfaces of the non-dimensional velocity distribution function within a normal shock wave with upstream Mach number $M = 2.5$ corresponding to an iso-value of $f = 1E-3$ obtained using various methods.

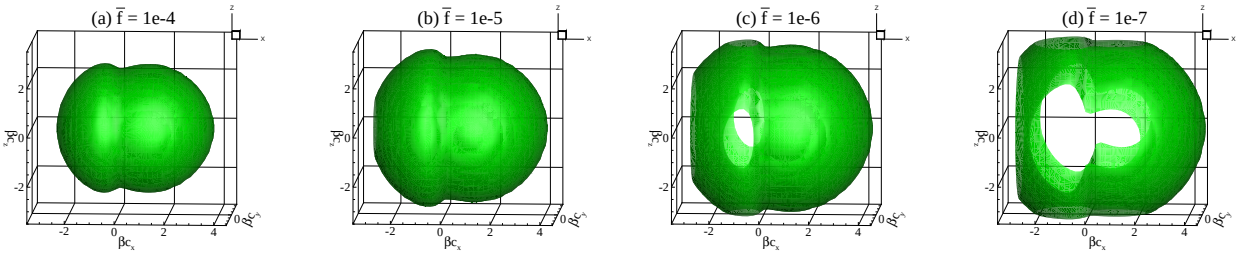

FIGURE 6. Iso-surfaces of the non-dimensional velocity distribution function within a normal shock wave for M = 2.5 obtained using the ES-BGK method and corresponding to various iso-values.

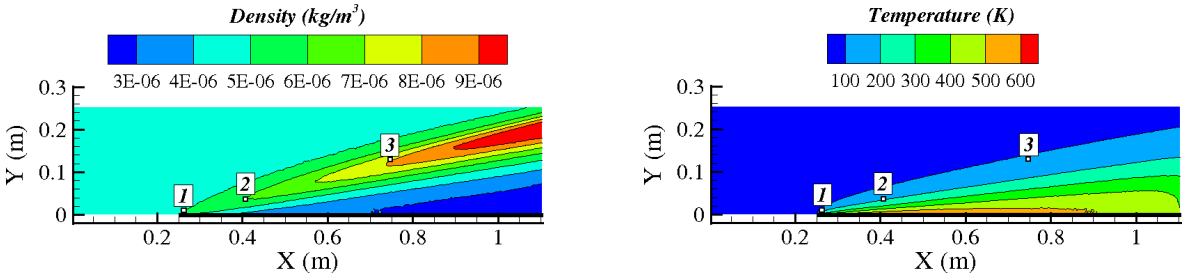

FIGURE 7. Density and Temperature contours of two-dimensional flow of nitrogen past a flat plate at M = 10 with the three VDF locations indicated

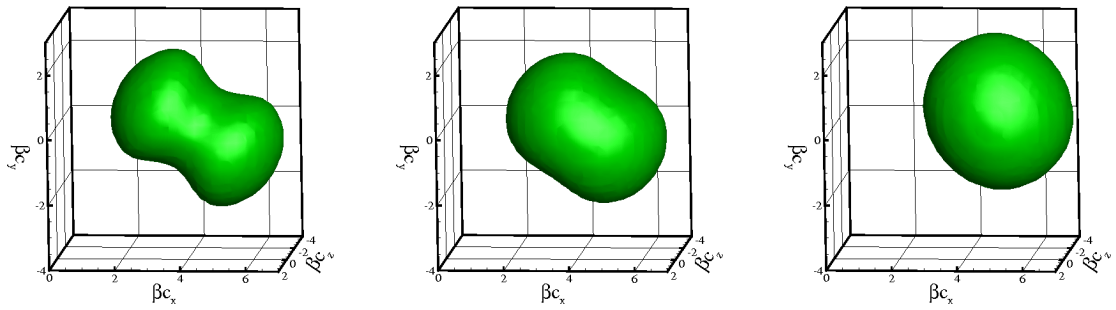

FIGURE 8. Comparison of isosurfaces of the velocity distribution function at (left) Location 1, (middle) Location 2, (right) Location 3 corresponding to an isovalue of $f = 1E-3$

REFERENCES

1. E. Bethal, C. Johnson, C. Hansen, and et.al, *SciDAC Review* **8**, 24–33 (2008).
2. U. Bordoloi, D. Kao, and H. Shen, *Data Science Journal* **3**, 153–162 (2004).
3. K. Potter, J. Krueger, and C. Johnson, "Towards the Visualization of Multi-Dimensional Schotastic Distribution Data," in *International Conference on Computer Graphics and Visualization*, 2008.
4. G.A.Bird, *Molecular Gas Dynamics and the Direct Simulation of Gas Flows*, Oxford University Press, New York, 1994.
5. L. Holway, *Physics of Fluids* **9**, 1658 (1966).
6. L. Mieussens, and H. Struchtrup, *Physics of Fluids* **16**, 2797–2813 (2004).
7. S. Chapman, and T. Cowling, *The Mathematical Theory of Non-uniform Gases*, Cambridge University Press, 1991.
8. H. Mott-Smith, *Physical Review* **82**, 885–892 (1951).
9. S. Chigullapalli, A. Venkattraman, M. Ivanov, and A. Alexeenko, *Journal of Computational Physics* **229** (2010).
10. M.S.Ivanov, A.V.Kashkovsky, S.F.Gimelshein, G.N.Markelov, A.A.Alexeenko, Ye.A.Bondar, G.A.Zhukova, S.B.Nikiforov, and P.V.Vaschenkov, "SMILE System for 2D/3D DSMC Computations," in *25th International Symposium on Rarefied Gas Dynamics*, St.Petersburg, Russia, 2006, pp. 539–544.